LAWRENCE
LIVERMORE
NATIONAL
LABORATORY

UCRL-CONF-203577

Downscattered Neutron Imaging

M. Moran, S. Haan, S. Hatchett, J. Koch, C. Barrera, E. Morse

April 16, 2004

The 15th Topical Conference on High-Temperature Plasma Diagnostics
San Diego, CA, United States
April 19, 2004 through April 22, 2004

UCRL-CONF-203577

Downscatered Neutron Imaging

Michael Moran, Steven Haan, Stephen Hatchett, and Jeffrey Koch
Lawrence Livermore National Laboratory

and

Carlos Barrera and Edward Morse
University of California, Berkeley

Images with 14-MeV neutrons of ICF D,T fusion show the regions of most intense fusion burn, while images based on lower-energy "downscattered" neutrons can reveal regions of nonburning D,T fuel . The downscattered images can help to understand ICF implosion dynamics. Recording downscattered images is difficult because the images are relatively weak, and because they may be obscured by residual "afterglow" of more intense 14-MeV images. The effect of "afterglow" can be estimated by adding a sequence of images for neutron energies from 14 MeV down to the downscattered energy of interest. The images will be subject to decay factors which depend on the time response of the neutron scintillator. Preliminary analyses suggest that afterglow will not prevent the recording of useful downscattered images.

Images of burning ICF (Inertial confinement Fusion) targets depend on the neutron energies that are recorded by the neutron camera. With D,T fusion, conventional images integrate the entire neutron spectrum from the 14.1-MeV peak down to 2.5-MeV (from D,D fusion), and below. Images of this kind are dominated by a small bright core near the center of the compressed target that is due mostly to neutron energies in the 14.1-MeV peak. Neutron energies between 14.1 MeV and 2.5 MeV result from elastic scattering of 14-MeV neutrons by deuterium and tritium throughout the volume of the target. Images based on these "downscattered" neutron energies would show the spatial distribution of deuterium and tritium throughout the target. Such images, when compared with the 14.1-MeV images of fusion burn, would reveal regions of nuclear fuel which are not contributing to the fusion yield of the target. In this way, downscattered images would provide direct evidence of the efficacy of fuel compression in an ICF target.

Images of downscattered neutrons will become feasible in high-yield experiments at the NIF (National Ignition Facility), even for targets which fail to achieve nuclear ignition. Hydrodynamic modeling of a sub-ignition ICF target has been used previously to demonstrate that images of downscattered neutrons can reveal the spatial distribution of non-burning deuterium and tritium fuel in regions that surround the hot compressed core where fusion reactions are most intense. The surrounding regions of nonburning fuel were associated with a sixth-order Legendre polynomial perturbation that was imposed on a spherical cryogenic NIF target, and which was large enough to reduce the yield from 17 MJ to 30 kJ. The model demonstrated that images based on downscattered neutrons showed clearly the symmetry of the perturbation which had been imposed on the system.

The image analysis demonstrated the potential value of imaging downscattered neutrons, but it raises the question of whether such measurements are feasible. Experimentally, imaging downscattered neutrons is difficult because their source intensities are, roughly, 100 to 1000 times less intense than the corresponding 14-MeV images. Neutron imaging systems are fairly simple in that they are based on a neutron pinhole and a scintillation detector/camera which records the pinhole image. In practice, a number is features such as pinhole design, neutron shielding, image magnification, detector sensitivity and time response can be chosen the optimize the image quality expected from a specific experiment. In the present case, a long imaging line-of-sight and a gated neutron imager also provide energy resolution that make possible the recording of images within specific bands of energies. If the downscattered images satisfy basic requirements of feasibility, then it is likely that the experimental parameters can be designed to record the desired images.

The feasibility of recording downscattered -neutron images depends on the signal-to-noise characteristics of the images. A simple analysis of the expected noise characteristics, based on a

rudimentary imaging system, can provide useful guidance to the design of a successful downscattered-neutron imaging system. This approach, working with the same hydrodynamic modeling results, together with a nominal pinhole design and a typical neutron detector efficiency, can estimate the signal-to-noise characteristics that can be expected for the neutron images. In this case, where only a small fraction of neutrons is detected, the noise characteristics of a single imaging pixel can be described by Poisson statistics. Simply stated, this means that the uncertainty (i.e., noise) associated with a specific pixel varies with the square root of the image intensity at that pixel.

The overall neutron detection efficiency of the imaging system will determine the image intensity, and thus the noise characteristics of a given pixel. The detection efficiency depends mostly on the neutron pinhole and on the detector design. The imaging detector itself can be expected to have a detection efficiency of about 0.1 - regardless of the specific choice of neutron scintillator. Lower efficiencies cause undesirable reduction in sensitivity, and higher efficiencies will introduce image distortion from multiple neutron interactions. The design of the neutron pinhole offers some flexibility in a tradeoff between spatial resolution and detection efficiency.

The analysis here is based on hypothetical ideal pinholes with diameters of 5 μm and 20 μm. These choices are based on the requirement for spatial imaging in NIF neutron imaging experiments (5 μm), and the spatial resolution which appears to be feasible with current imaging systems (≈ 20 μm). A variety of so-called "coded apertures" have been used with varying degrees of success in an attempt to improve on the efficiency of a simple pinhole without sacrificing the loss of resolution that accompanies the use of a larger pinhole. The present analysis will include some consideration of a specific type of coded aperture: a 10 by 10 array of single apertures with, either, 5-μm or 20-μm diameters. This analysis is not intended to study the feasibility of building and using a specific imaging system, and is intended only to estimate the expected noise characteristics of the hypothetical recorded images.

The hypothetical imaging system consists of a line-of-sight with either a 5-μm, 20-μm pinhole, or an array of them, located 10 cm from the target. The image is recorded in detector pixels (depending on the pixel size and system magnification) which correspond to images of 5 μm "pixels" at the source. Thus, 5-μm pixels at the source are imaged into corresponding single detector pixels. The solid-angle fraction of the pinhole ($\approx 1.5 \times 10^{-10}$), together with at detector neutron efficiency of 0.1 combine to provide an overall detection efficiency of 1.5×10^{-11} detected neutrons per source neutron. The corresponding efficiency for a 20-μm pinhole is sixteen times greater (2.4×10^{-10}); and the use of a 10x10 array boosts these efficiencies by another factor of 100.

Individual images neutrons emitted with energies within 1-MeV bins from 14 MeV to 6 MeV were extracted from the hydrodynamic model of the same perturbed ICF capsule mentioned above. Figure 1 shows the corresponding neutron images, with corresponding plots of time of flight vs. neutron energy (blue) and neutrons/ns for a detector located 25 metes from the source. The plots and images indicate that the downscattered images will be recorded with neutron intensities as much as three decades smaller than the 14-MeV image. The 14-MeV image is so much brighter that its residual image (about 250 ns later)could interfere with recording the downscattered neutron image in the 6-7 MeV bin.

As a first step to modeling the image actually recorded in the 6-7 MeV energy window at 250 ns after arrival of the 14.1 MeV neutrons, an image is constructed which represents the net sum of residual images from higher-energy (i.e., earlier) bins. The original images first were binned into a 16x16 array of 5μm pixels with intensities representing the brightness of the original image. Before summing the images brightness of the earlier images was reduced in intensity by a factor corresponding to the scintillation decay of the scintillator BC-422. For example, the 14-MeV image was multiplied by a decay factor of 2.8×10^{-4}.

Figure 2 show the resulting images. Here, the raw binned 14-MeV and 6-7 MeV images are shown, along with the image which represents the decay-weighted sum of images from all energy bins. The fourth image shows the image which would result from subtracting the (presumably recorded) 14-MeV image multiplied by its decay factor. The final image is "contaminated" by small contributions from other energies, but the rapid decay of the scintillator makes these contributions negligible. Of course, this result ignores degradation of the images by statistical noise associated with finite signal amplitudes.

In order to study the effects of noise on the images, the 14-MeV and "weighted sum" images in Fig. 2 were mapped into new "noisy" images. Here, each pixel was assigned a new value, according to a Poisson distribution whose mean value was given by the intensity of the original pixel. Then, the "Poissoned" 14-MeV image, multiplied by its decay factor, was subtracted from the "weighted sum". This procedure produces a model of the 6-7-MeV image which would be extracted from the data.

These images with Poisson statistics are shown in Fig.3. The images clearly show degradation from statistical noise, but basic features of the images still are evident. The appearance of the images can depend strongly on their method of display. The "pixel" images in Fig. 3 show point-by-point brightnesses of pixels in the final image. The "difference" image, while still retaining the basic original features is very fuzzy. The "contour" display of Fig. 3 shows the same data, now displayed with the "contour" plotting option in Microsoft Excel. The fitting routines which are embedded in the contour plotting option seem to be able to infer correctly feature sin the image which are not evident in the "pixel display.

These results indicate that, based on raw detector statistics, recording of downscattered neutron images is feasible. Further analysis is necessary before a final conclusion can be drawn , but

these initial results are promising. Issues such as realistic pinhole point spread functions, spatial resolution of detectors and energy dependence of detector sensitivity all will introduce addition (and hopefully small) distortions to the images. Analysis of these issues will continue and ultimately are intended to be used as a guide to the design of a downscattered neutron imaging system for NIF ignition experiments. This work was performed under the auspices of the U.S. Department of Energy by the University of California, Lawrence Livermore National Laboratory under contract No. W-7405-Eng-48.

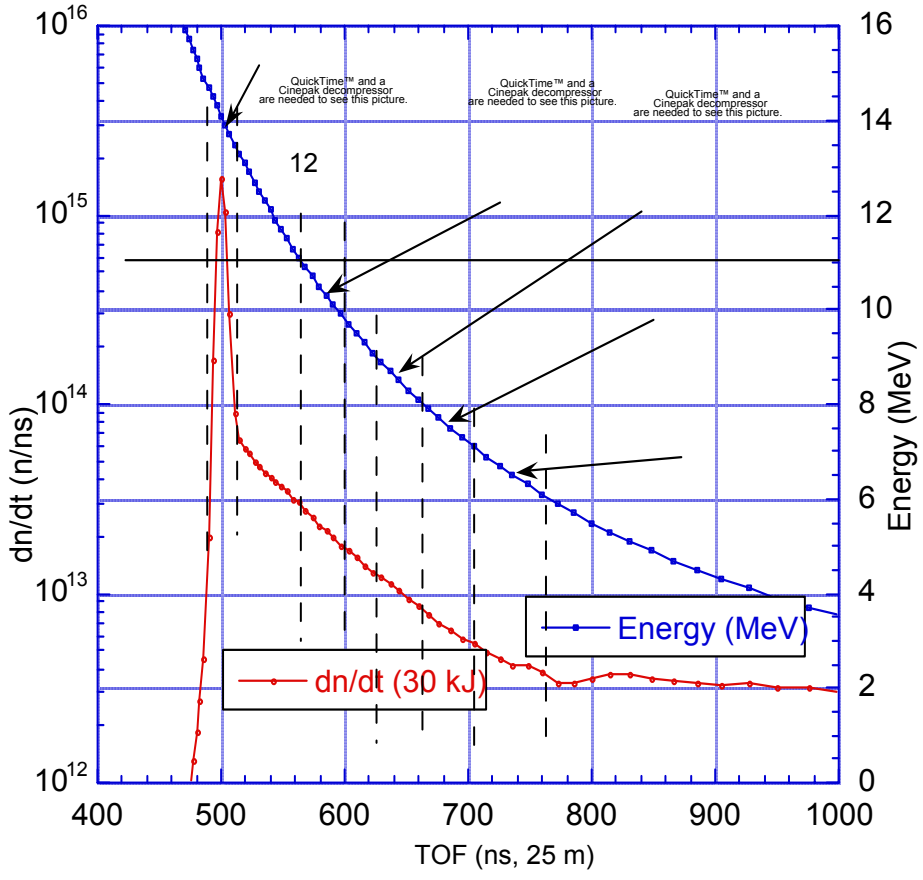

Figure 1 Energy-dependent neutron images

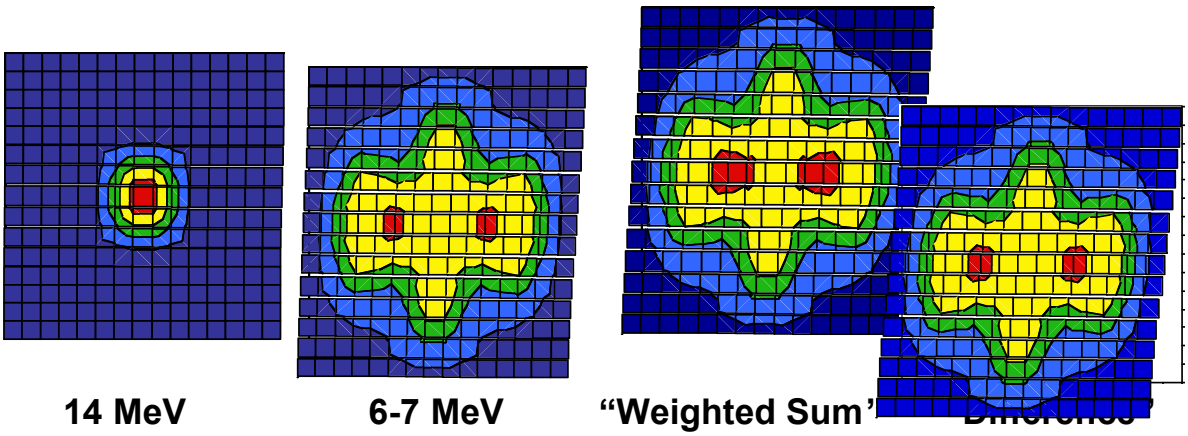

Figure 2 Neutron images, sum, and difference

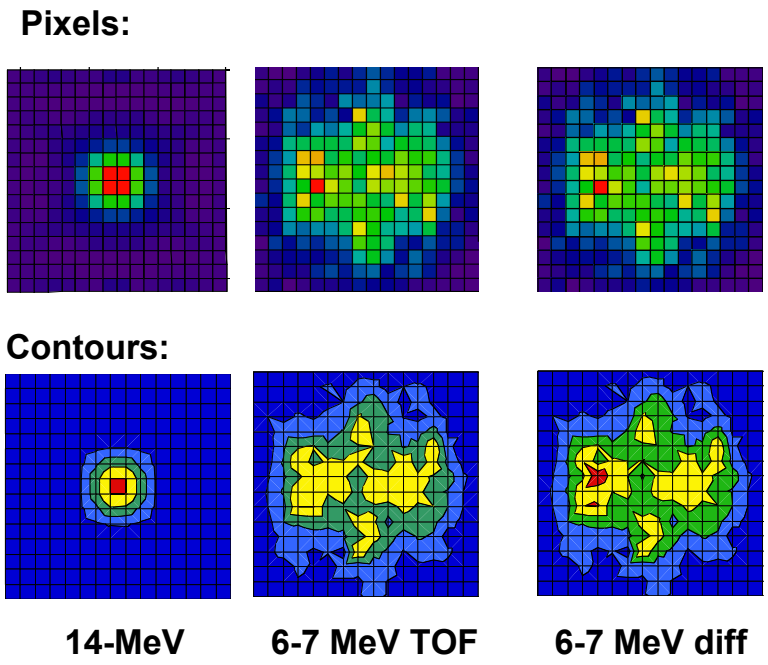

Figure 3 14-MeV, 6-7 MeV, and difference sums, with Poisson statistics